Asymmetric Charge Carrier Transfer and Transport in Planar Lead Halide Perovskite Solar Cells

Weidong Xu, Tian Du, Michael Sachs, Thomas J. Macdonald, Jiaying Wu, Chieh-Ting Lin, James R Durrant

Imperial College London

The Centre for Plastic Electronics

Introduction

Understanding the extraction of charge carriers from perovskite photoactive layer is critical to optimizing the design of perovskite solar cells. Herein we focus on using a simple time-resolved photoluminescence (TRPL) method to characterize charge transport across bulk perovskite and charge transfer from perovskite to interlayers, elucidating their dependence on film thickness, grain boundary (GB) and interlayers. Particularly, with asymmetric laser excitation, we selectively probe charge transport by generating charges away from heterojunction interface and charge transfer by generating charges near the interface, ultimately correlate these properties with device performance. We observed that whilst both kinetics affected by film thickness and GBs, there is an asymmetry between electron and hole transport across bulk perovskite as well as electron and hole transfer from perovskite to interlayers.

Asymmetric excitation of perovskite samples with 404nm laser

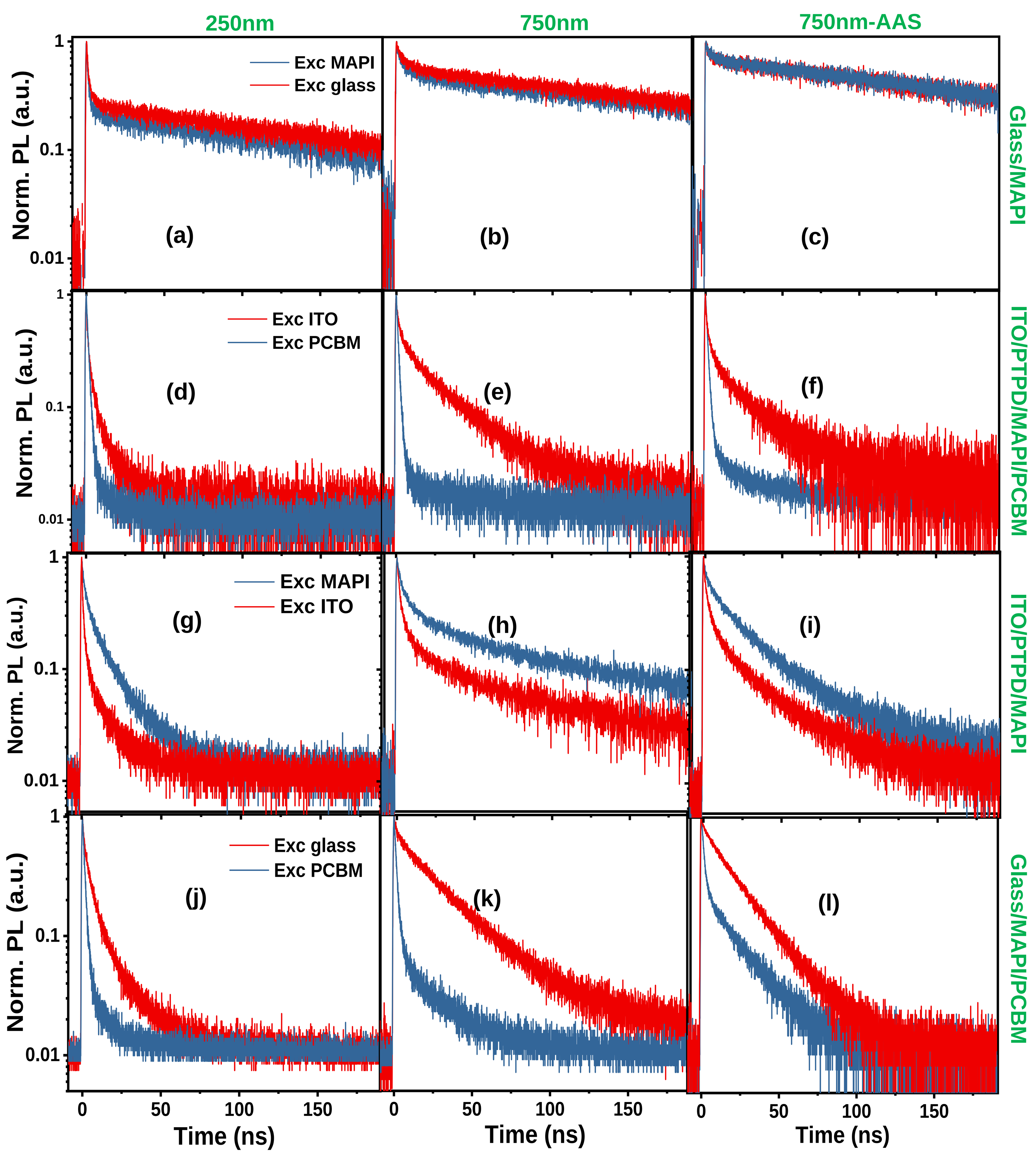

1, Neat MAPI films do not show much difference in long time decay meaning they have same majority of bimolecular recombination kinetics. However, the first fast decay associated to the defects illustrates that the films have different trap densities.

AAS: Aerosol assisted solvent annealing treatment.

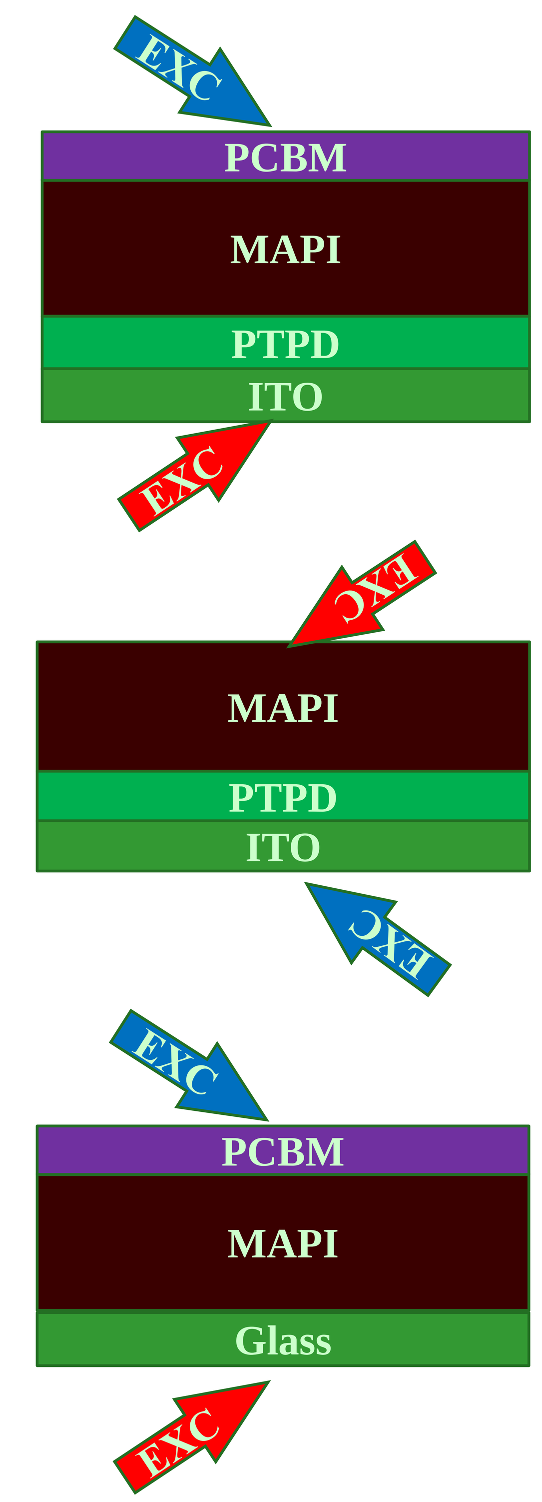

Figure 3, TCSPC of (a) (d) (g) (j)250nm, (b) (e) (h) (k)750nm and (c) (f) (i) (l)AAS-750nm MAPI films on glass, ITO/PTPD/MAPI/PCBM, ITO/PTPD/MAPI and Glass/MAPI/PCBM excited with 6mW/cm² 404nm pulsed laser from two sides.

2, Decay kinetics show faster when excited from CTL/MAPI side than its opposite side, indicating transport transfer dominates the former decays while charge transport dominates the later ones.

3, Thick MAPI shows a larger difference for different surface excitation due to the longer transport distance comparing with thin MAPI. However, the difference is decreased when GBs were removed by AAS, suggesting faster and more efficient charge transport in AAS-750nm samples.

4, Decays from excitation on PTPD/MAPI surface is always slower than PCBM/MAPI surfaces, indicative of slower charge transfer from MAPI to PTPD than PCBM.

Device performance and morphology: Evidence of grain boundaries

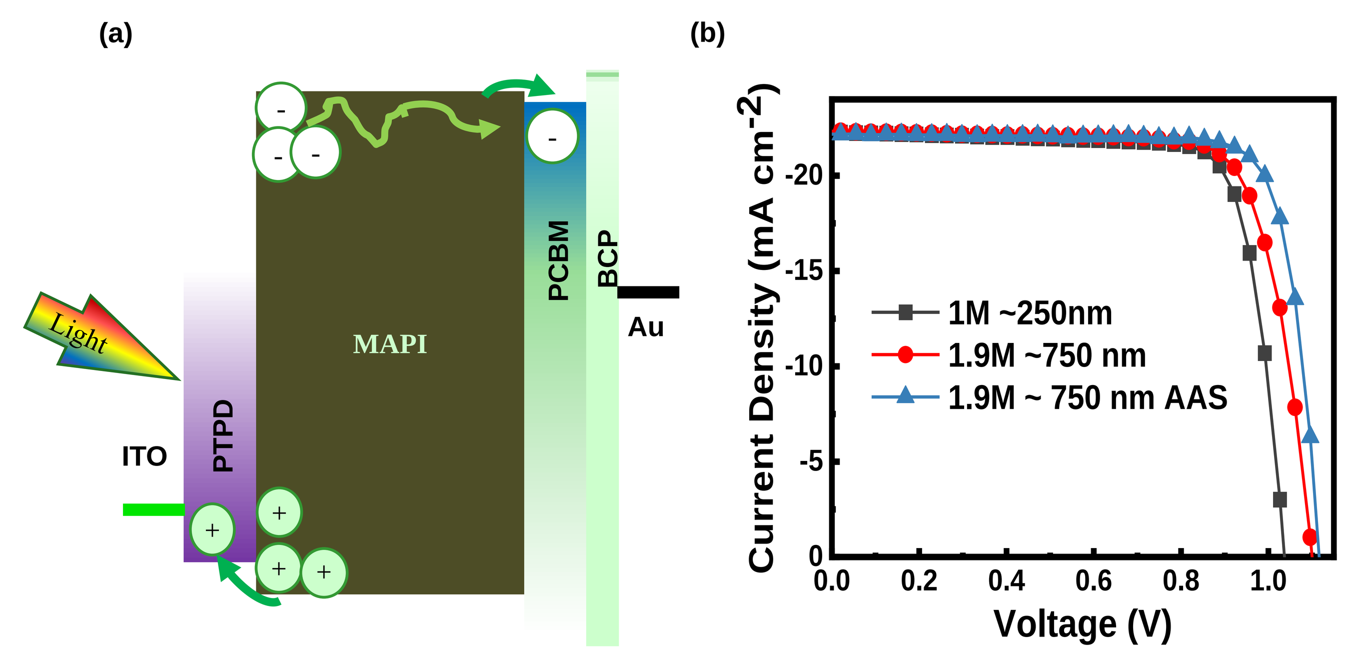

Figure 1, device a) energy diagram and device performance b) J-V curve 250nm-Norm 750nm-AAS 750nm

By making perovskite thick, V_{OC} is increased but FF is dropped due to the formation of GBs in the vertical way.

After AAS, GBs are removed, V_{OC} and especially FF are further increased.

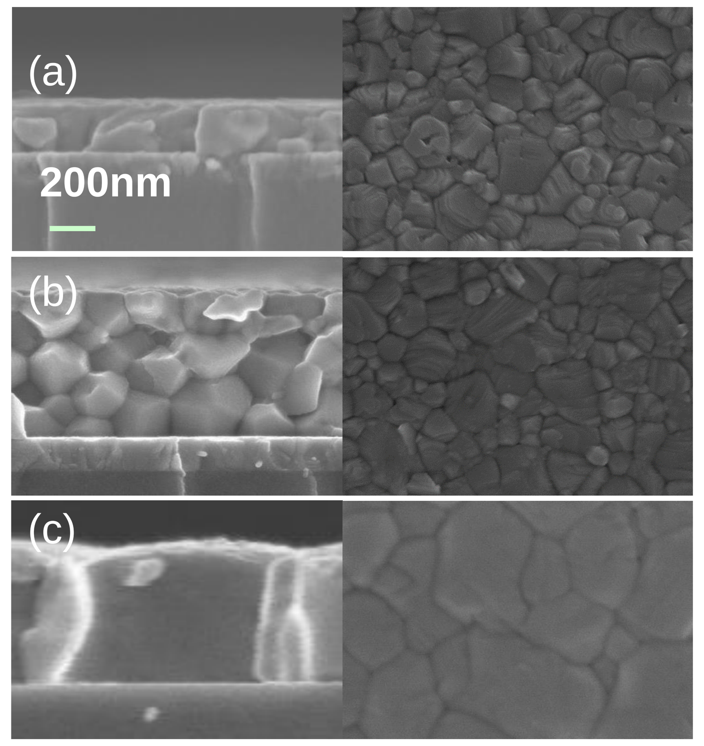

Figure 2, morphology: SEM: a)cross section 250nm b) cross section 750nm c) cross section AAS 750nm d)norm SEM 250nm e) norm SEM 750nm f) norm SEM AAS-750nm

Device performance

V_{OC} increases all the time while FF drops first then rises to higher value

Perovskite Thickness/nm	J_{SC}/mA cm^{-2}	V_{OC}/V	FF	PCE/%
250	22.2	1.04	0.79	18.2
750	22.3	1.10	0.77	18.9
AAS-750	22.2	1.11	0.81	20.1

Steady-state PL measurement of neat perovskite films: film property

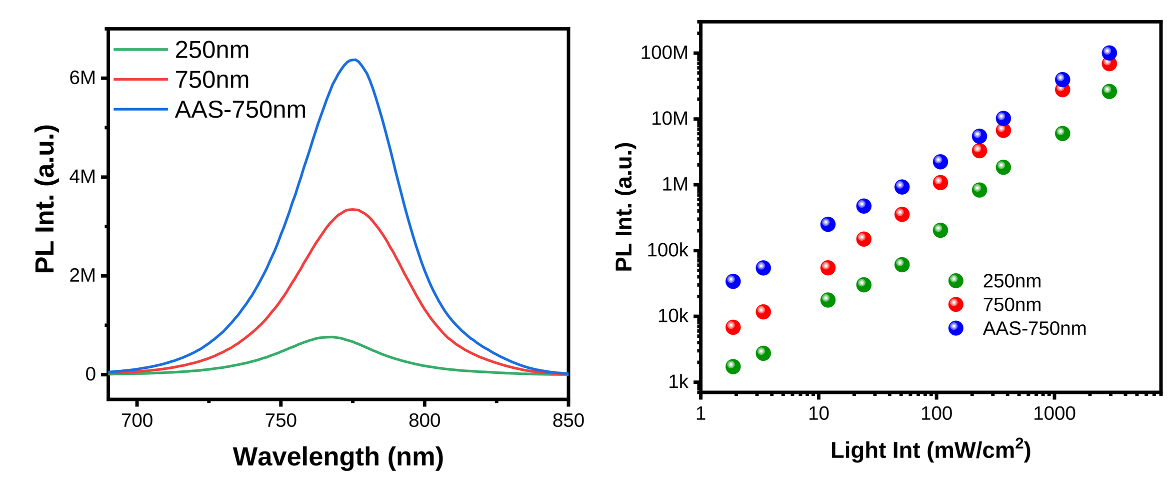

Figure 4, steady-state PL spectrum, as well as light intensity dependent PL measurement of 250nm, 750nm and AAS-750nm neat perovskite on glass substrate.

Non-radiative recombination loss: 250nm>750nm>AAS-750nm

Indicative of the same order in terms of trap density

Homogenous excitation from the bulk perovskite with 635nmnm laser

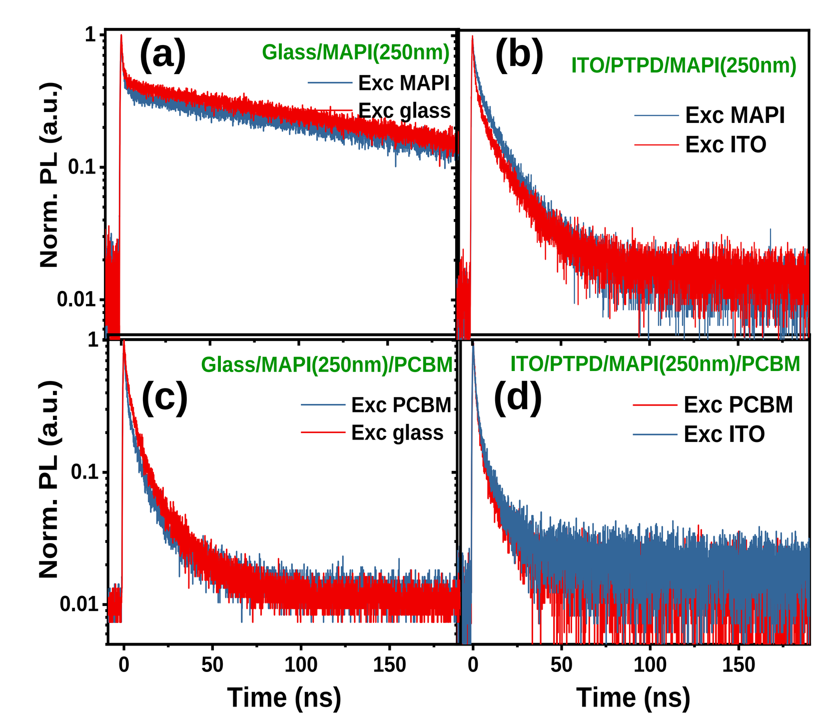

Figure 5, Double side excited TRPL of thin MAPI film (250nm) based samples: a)glass/MAPI, b)ITO/PTPD/MAPI, c)glass/MAPI/PCBM, d)ITO/PTPD/MAPI/PCBM, with 5.3mW/cm² 637nm pulsed excitation.

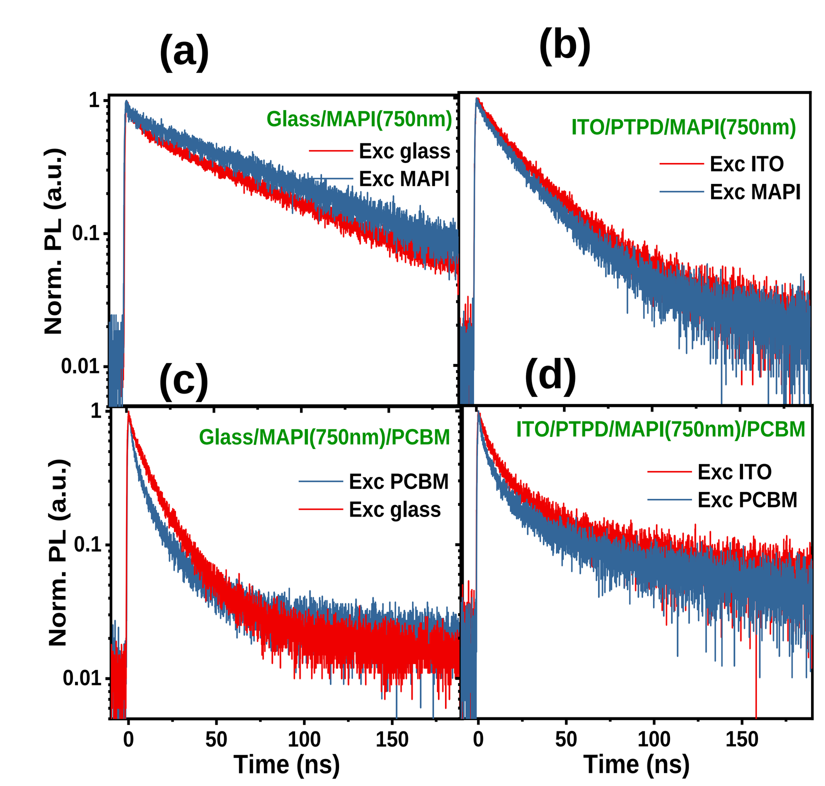

Figure 6, Double side excited TRPL of thick MAPI film (750nm) based samples: a)glass/MAPI, b)ITO/PTPD/MAPI, c)glass/MAPI/PCBM, d)ITO/PTPD/MAPI/PCBM, with 5.3mW/cm² 637nm pulsed excitation.

1-D diffusion mode is used to calculate the mobility

$$\frac{\partial p(x,t)}{\partial t} = D\frac{\partial^2 p(x,t)}{\partial x^2} - \frac{p(x,t)}{\tau} \qquad L_D = \sqrt{D\tau} \qquad u = \frac{q}{kT}\cdot\frac{L^2}{t}$$

Perovskite thickness	Bilayer lifetime t2 (ns)	Neat film lifetime t2 (ns)	Electron mobility (cm² V⁻¹ S⁻¹)	Hole mobility (cm² V⁻¹ S⁻¹)
250nm	1.27	132.21	1.7	1.4
750nm	4.83	260.67	9.4	3.4
750nm-AAS	3.1	298.23	11.3	6.3

Conclusion:

In summary, by simply growing perovskite thicker, traps can be largely reduced therefore contributing to a huge improvement in V_{OC}. However, by using asymmetric excitation in surface quenching TRPL method, we found thick MAPI suffers from imbalanced charge transport within the bulk between electron and hole due to GBs hinders more on hole transport rather than electron. By employing AAS, GBs in the thick MAPI can be effectively eliminated, a more balanced and faster charge transport is obtained. These properties facilitate charge extraction in total, though slow hole transfer still limits the efficiency. Finally, PSC with 20% is achieved mainly due to the increase in FF.